

## INFLUENCE OF Dy DOPING ON THE PROPERTIES OF BiFeO<sub>3</sub>

The aim of this research was to fabricate and study the properties of Bi<sub>1-x</sub>Dy<sub>x</sub>FeO<sub>3</sub> (for x = 0, 0.05, 0.07, 0.1) ceramics materials. Simple oxide powders Bi<sub>2</sub>O<sub>3</sub>, Dy<sub>2</sub>O<sub>3</sub> and Fe<sub>2</sub>O<sub>3</sub> were used to fabricate Bi<sub>1-x</sub>Dy<sub>x</sub>FeO<sub>3</sub> ceramics by mixed oxide method followed by free sintering. The study presents changes in microstructure and crystal structure as well as in dielectric properties and magnetic properties caused by modification of BiFeO<sub>3</sub> with dysprosium dopant.

*Keywords:* Doped BiFeO<sub>3</sub>, mixed-oxide method, ceramics, Dy<sup>3+</sup>

### 1. Introduction

Multiferroic materials have recently attracted wide attention because they show both ferromagnetic and ferroelectric ordering in a single phase and also because of the promising multifunctional device applications in information storage, sensor, spintronics, multi-states memory, etc. and fascinating basic physics [1,2]. Some of the multiferroic materials possess simultaneously ferroelectric and ferromagnetic properties only in relatively low temperature [3].

The bismuth ferrite (BiFeO<sub>3</sub>) is one of the rare multiferroic materials with both ferroelectric behavior (Curie temperature  $T_C = 830^\circ\text{C}$ ) and antiferromagnetic ordering (Neel temperature  $T_N = 380^\circ\text{C}$ ) above the room temperature [4]. The structure of BiFeO<sub>3</sub> is a distorted rhombohedral perovskite having R3c space group with a unit cell parameter  $a = 0.5643\text{ nm}$  and  $\alpha = 59.3488^\circ$  [5]. BiFeO<sub>3</sub> has a spin-modulated cycloidal magnetic structure with modulation period of  $\sim 62\text{ nm}$ . Bismuth ferrite has attracted lots of attention in recent years because its temperature of phase transitions (of both magnetic and electric ordering) is above room temperature which enables using it in multiferroic devices working at a room temperature (for example, magnetoelectric random access memory (MeRAM) elements) [6].

Although bismuth ferrite BiFeO<sub>3</sub> has very good physical properties, there are still attempts to improve the ferroelectric and ferromagnetic properties [7]. Doping of BiFeO<sub>3</sub> is interesting because it enables changes in the properties of the result material therefore partial substitution of Bi<sup>3+</sup> ions with rare earth ions results in improved multiferroic properties of BiFeO<sub>3</sub> [8,9]. The structure, the electrical and magnetic properties of the

obtained ceramics were systematically studied and the results are discussed in detail.

### 2. Experimental part

The dysprosium modified BiFeO<sub>3</sub>:Dy<sup>3+</sup> ceramics was obtained by using the conventional mixed-oxide processing technique starting from stoichiometric amounts of Bi<sub>2</sub>O<sub>3</sub> (Sigma – Aldrich, 99,9%), Fe<sub>2</sub>O<sub>3</sub> (Sigma – Aldrich, 99,9%) and Dy<sub>2</sub>O<sub>3</sub> (Sigma – Aldrich, 99,9%) reagents. The mixture of the simple compositions was milled by Fritsch-type planetary ball mill for 24 h (immersed in wet ethanol). The role of grinding media was made of zirconium-yttrium (3Y – TZP) balls with diameter  $d = 10\text{ mm}$ . Mixtures of the powders were synthesized by calcination method at a temperature of  $800^\circ\text{C}$  for 3h. Compaction was carried out by the free sintering method at a high temperature  $T = 880^\circ\text{C}$  for 3 h. The furnace temperature increase rate was  $v = 5^\circ\text{C} / \text{min}$ .

The structure of the samples was studied using PANalytical X-Pert Pro diffractometer with Cu lamp ( $\lambda = 0.154\text{ nm}$ ).

The chemical composition of Bi<sub>1-x</sub>Dy<sub>x</sub>FeO<sub>3</sub> ceramic samples was examined by scanning electron microscopy (SEM) using the HITACHI S-4700 microscope with the microanalysis system EDS (Energy Dispersive Spectroscopy) EDS-NORAN Vantage. The measurements were performed on the fractured surface of BiFeO<sub>3</sub>:Dy<sup>3+</sup> ceramics.

The samples are tested using Mössbauer's spectroscopy. A constant acceleration POLON spectrometer was used. As a source of gamma quanta with energy  $E = 14.4\text{ keV}$ , the <sup>57</sup>Co deposited in Rh crystalline matrix was used.

\* UNIVERSITY OF SILESIA, INSTITUTE OF TECHNOLOGY AND MECHATRONICS, FACULTY OF COMPUTER SCIENCE AND MATERIAL SCIENCE, 12 ŻYTANIA STR., 41-205 SOSNOWIEC, POLAND

\*\* LUBLIN UNIVERSITY OF TECHNOLOGY, INSTITUTE OF ELECTRONICS AND INFORMATION TECHNOLOGY, 38A NADBYSTRZYCKA STR., 20-618 LUBLIN, POLAND

\*\*\* DEPARTMENT OF GEOTECHNICS, CIVIL ENGINEERING AND ARCHITECTURE FACULTY, LUBLIN UNIVERSITY OF TECHNOLOGY, 40 NADBYSTRZYCKA STR., 20-618 LUBLIN, POLAND

# Corresponding author: jolanta.dzik@us.edu.pl

The electrical properties of  $\text{Bi}_{1-x}\text{Dy}_x\text{FeO}_3$  were studied using a computer-controlled wide frequency Precision LCR (inductance (L), capacitance (C) and resistance (R)) meter Agilent E4980A.

### 3. Results and discussion

Based on the density studies, it can be stated that the increase in dysprosium resulted in increased density which is as follows:  $7.2755 \text{ g/cm}^3$  (for  $\text{Bi}_{0.95}\text{Dy}_{0.05}\text{Fe}_2\text{O}_3$ ),  $7.3571 \text{ g/cm}^3$  (for  $\text{Bi}_{0.93}\text{Dy}_{0.07}\text{Fe}_2\text{O}_3$ ) and  $7.3874 \text{ g/cm}^3$  (for  $\text{Bi}_{0.9}\text{Dy}_{0.1}\text{Fe}_2\text{O}_3$ ).

In order to determine the effect of the dopant on the crystal structure of the ceramics, XRD studies were carried out. XRD data of the  $\text{Bi}_{1-x}\text{Dy}_x\text{FeO}_3$  ceramics obtained at a room temperature are presented in Fig. 1. The best fit to the measured data was obtained with the pattern 01-082-1254. The unit cell parameters are:  $a = b = 0.5564 \text{ nm}$ ,  $c = 1.3817 \text{ nm}$  for  $x = 0.1$ ,  $a = b = 0.5562 \text{ nm}$ ,  $c = 1.3817 \text{ nm}$  for  $x = 0.07$  and  $a = b = 0.5568 \text{ nm}$ ,  $c = 1.3833 \text{ nm}$  for  $x = 0.05$  (a trigonal system that is actually a rhombohedral cell of a hexagonal system [10]). Diffraction lines coming from impurity phases are visible on diffractograms but their intensities are rather small. The occurrence of weak lines for  $2\theta = 27\text{--}30^\circ$  not connected with the  $\text{BiFeO}_3$ -type structure is caused by the presence of a vestigial quantity of  $\text{Bi}_2\text{Fe}_4\text{O}_9$ . In addition, it was observed that with the increase in dopant content, the amount of  $\text{Bi}_2\text{Fe}_4\text{O}_9$  was reduced.

As proved by the EDS analysis, the obtained  $\text{Bi}_{1-x}\text{Dy}_x\text{FeO}_3$  ceramic materials were pure and homogeneous samples with low concentration of impurity phases or without any impurities. Table 1 shows the theoretical and experimental content of elements (calculation for simple oxides) for  $\text{Bi}_{1-x}\text{Dy}_x\text{Fe}_2\text{O}_3$  ceramics. It may be observed that small deviations from the theoretical composition have occurred but they do not exceed the value of 2.6%. It is consistent with the assumptions of the utilized method of investigation.

The surface of each ceramic sample was subject to a homogeneity study of the decomposition of the elements by the EPMA (Electron Probe MicroAnalysis) method. The “maps” shown in Fig. 2 show the distribution of the elements in the sample areas studied. Colored points confirm the presence of characteristic elements. The results of the study showed a uniform distribution of the constituent elements, i.e. bismuth, iron and dysprosium dopant. In addition, they confirmed the quality composition of the samples.

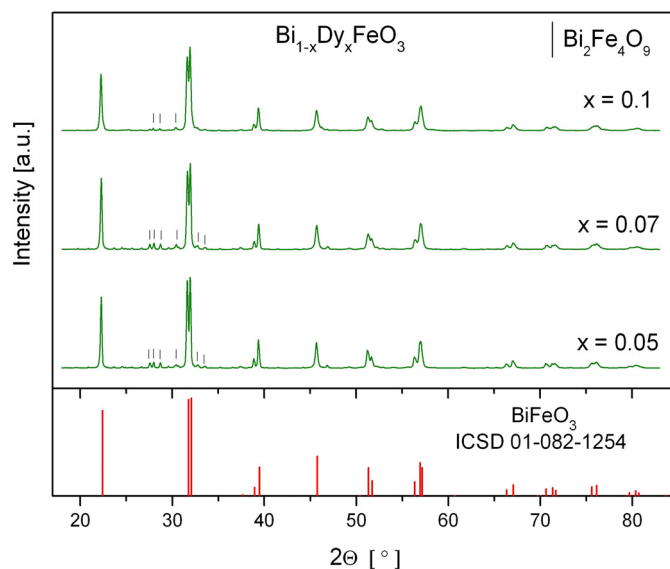


Fig. 1. X-ray diffraction patterns of  $\text{Bi}_{1-x}\text{Dy}_x\text{FeO}_3$  ceramics with  $x = 0.05$ ,  $0.07$  and  $0.1$ , respectively

The results of the Mössbauer spectroscopy studies for  $\text{Bi}_{1-x}\text{Dy}_x\text{Fe}_2\text{O}_3$  are presented in Fig. 3. The obtained Mössbauer spectra is symmetric six-line patterns typical of magnetically ordered systems. The Mössbauer spectra registered for received materials were fitted by hyperfine magnetic field distributions. The distributions were symmetric and Gaussian-like. Therefore it may be concluded that  $\text{Dy}^{3+}$  ions substitute  $\text{Bi}^{3+}$  ions randomly and disordered solid solutions was formed. In the central parts of the spectrum there are shown additional components derived from the phase pollutant  $\text{Bi}_2\text{Fe}_4\text{O}_9$ .

Before the electrical measurements, the silver electrodes were applied to both surfaces of the annealed bulk ceramic samples. The measurements of dielectric permittivity versus temperature were performed at frequencies in the range of 500 Hz-1000 Hz. Temperature characteristics of dielectric response for 1kHz of dysprosium modified ceramics are shown in Fig. 4a-c.

As can be clearly seen, the increase in the concentration of the dopant (from  $x = 0.05$  to  $x = 0.07$ ) leads to a decrease in the peak value of dielectric constant, while the temperature shift to higher values with increasing frequency. An increase in the concentration of dysprosium to  $x = 0.1$ , on the other hand, causes the dielectric permittivity to increase again. It was also observed that as the frequency increases, the dielectric constant decreases. The value of dielectric constant depends on some factors such as voids, grain boundaries and dipolar interaction [11].

TABLE 1

Theoretical and experimental content of element (calculation for simple oxide) for  $\text{Bi}_{1-x}\text{Dy}_x\text{FeO}_3$  ceramic

Formula	Oxide content by EDS measurement [%]			Theoretical content of oxides [%]			Content error [%]		
	$\text{Bi}_2\text{O}_3$	$\text{Dy}_2\text{O}_3$	$\text{Fe}_2\text{O}_3$	$\text{Bi}_2\text{O}_3$	$\text{Dy}_2\text{O}_3$	$\text{Fe}_2\text{O}_3$	$\text{Bi}_2\text{O}_3$	$\text{Dy}_2\text{O}_3$	$\text{Fe}_2\text{O}_3$
$\text{Bi}_{0.95}\text{Dy}_{0.05}\text{Fe}_2\text{O}_3$	71,246	3,05	25,702	70,98	3,13	25,89	0,373	2,623	0,731
$\text{Bi}_{0.93}\text{Dy}_{0.07}\text{Fe}_2\text{O}_3$	69,942	4,282	25,775	69,2	4,35	26,45	1,061	1,588	2,619
$\text{Bi}_{0.9}\text{Dy}_{0.1}\text{Fe}_2\text{O}_3$	67,972	6,143	25,884	67,95	6,21	25,84	0,032	1,091	0,17

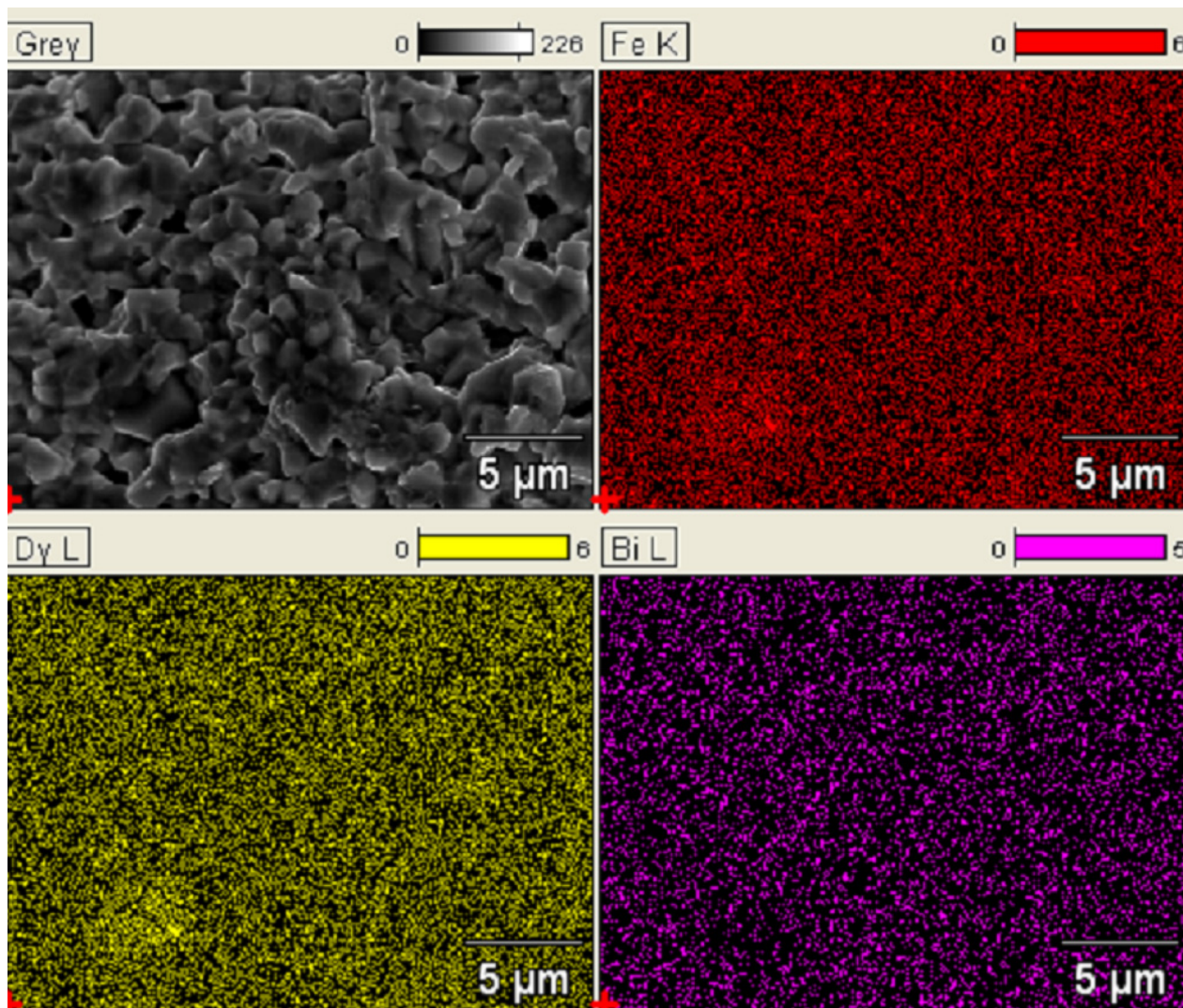


Fig. 2. Bi, Fe and Dy distribution maps in  $\text{Bi}_{0.9}\text{Dy}_{0.1}\text{Fe}_2\text{O}_3$  ceramics

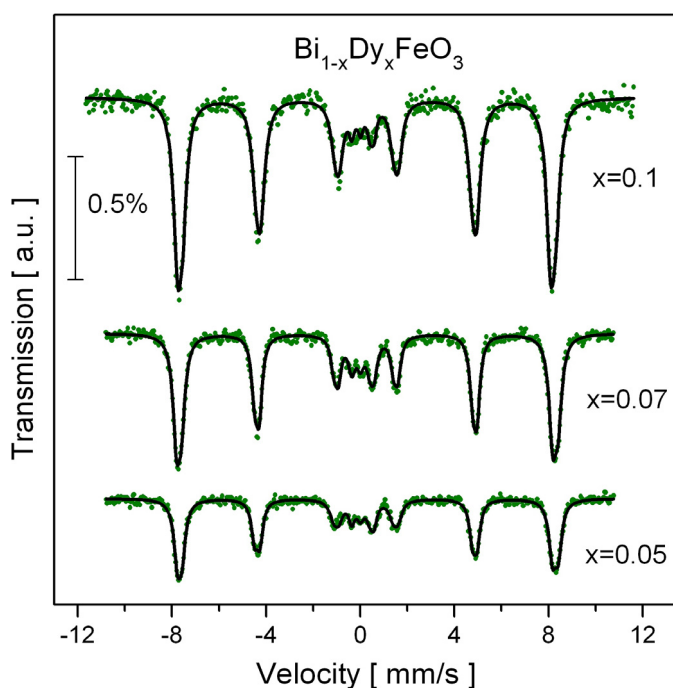


Fig. 3. Mössbauer spectrum of  $\text{Bi}_{1-x}\text{Dy}_x\text{FeO}_3$  ceramics

The  $\ln\rho(1000/T)$  dependence for the  $\text{Bi}_{0.9}\text{Dy}_{0.1}\text{FeO}_3$  is presented in Fig. 5. In the graph there are two characteristic inflection points where there is a change in the  $E_{\text{Act}}$  activation energy. Activation energies were calculated according to the Arrhenius law:

$$\rho = \rho_0 \exp\left(\frac{E_{\text{Act}}}{k_B T}\right)$$

where:  $k_B$  – Boltzmann constant,  $E_{\text{Act}}$  – activation energy,  $T$  – absolute temperature.

Fig. 6 shows the temperature dependence of electrical permeability  $\varepsilon$  as a function of the  $f$  frequency of the measuring field for the ceramic materials obtained. For all materials received, the electrical permeability value  $\varepsilon$  decreases as the measuring field frequency increases (for all measuring temperatures).

High electrical permeability values  $\varepsilon$  for lower frequencies can be explained in several ways. The cause may be the accumulation of spatial charge associated with heterogeneity of ceramic samples. This phenomenon is also explained by the fact that with the increase in frequency only electron polarization contributes

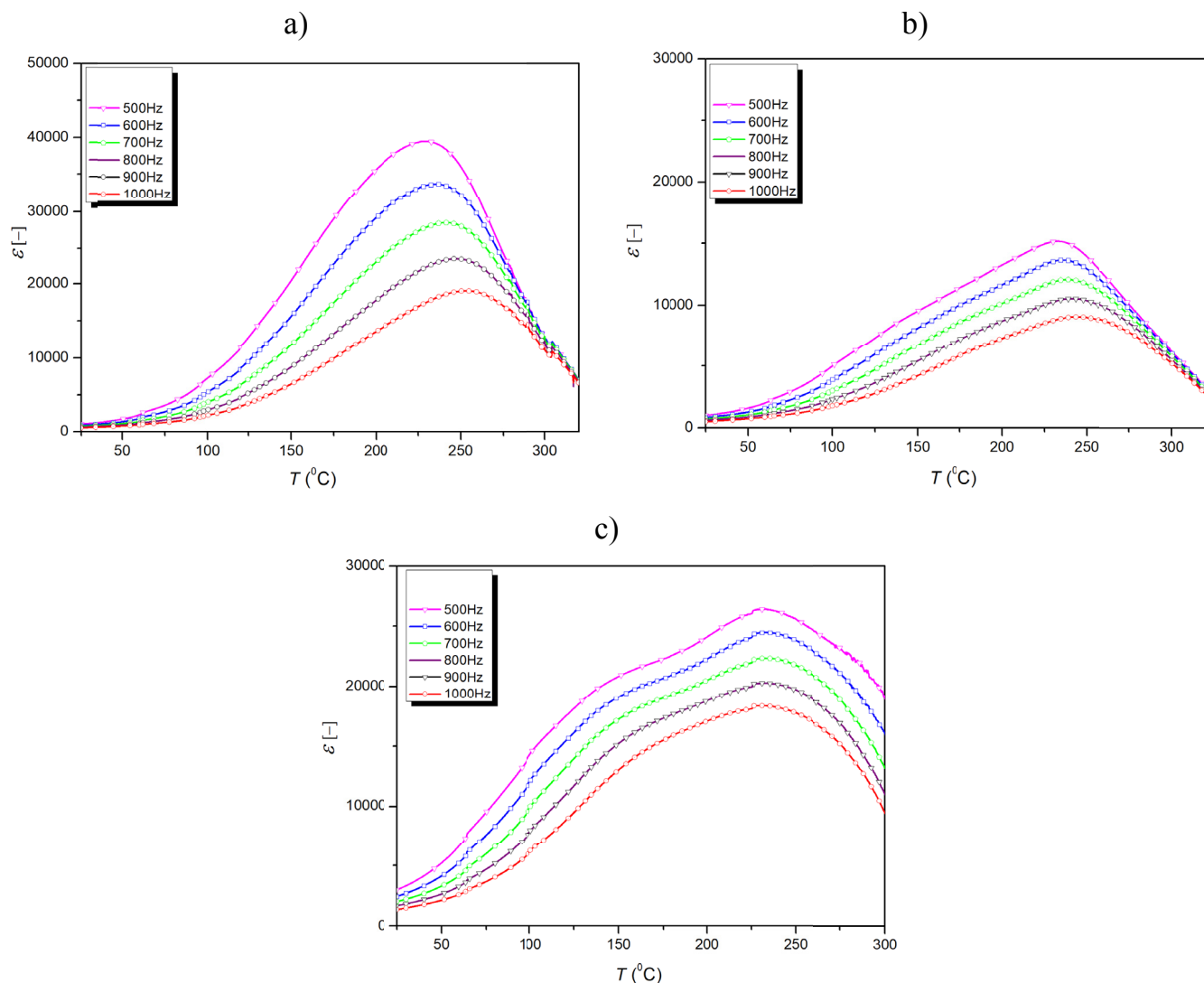


Fig. 4. Temperature dependences of dielectric permittivity for  $\text{Bi}_{0.95}\text{Dy}_{0.05}\text{Fe}_2\text{O}_3$  (a),  $\text{Bi}_{0.93}\text{Dy}_{0.07}\text{Fe}_2\text{O}_3$  (b) and  $\text{Bi}_{0.9}\text{Dy}_{0.1}\text{Fe}_2\text{O}_3$  (c)

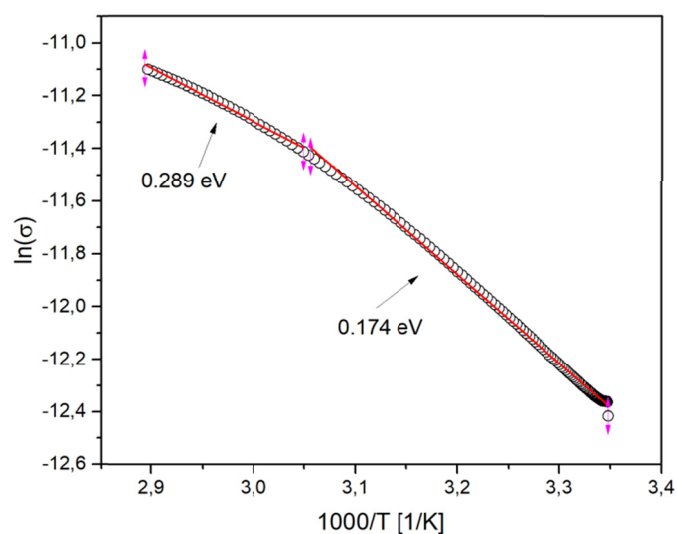


Fig. 5. The dependence of the  $\ln\rho(1000/T)$  for  $\text{Bi}_{0.9}\text{Dy}_{0.1}\text{FeO}_3$

to total polarization due to the fact that dipoles of other types have low mobility and cannot keep up with the rapid changes in the frequency of the electric field [12,13].

#### 4. Conclusions

$\text{Bi}_{1-x}\text{Dy}_x\text{FeO}_3$  ceramic powder was synthesized by mixed oxide method from the stoichiometric mixture of oxides, viz  $\text{Bi}_2\text{O}_3$ ,  $\text{Dy}_2\text{O}_3$  and  $\text{FeO}_3$ . EDS analysis confirmed the chemical composition and purity of the material received. For obtained materials, it was found that the experimental diffraction patterns corresponded to the rhombohedral structure described with R3c (No. 62) space group that is typical for bismuth ferrite. As a result of the research we received Mössbauer spectra composed of symmetric six-line patterns – typical for magnetically ordered materials. The values of electrical permeability  $\epsilon$  decrease as the measuring field frequency increases (for all measuring temperatures).

#### REFERENCES

- [1] A.R. Damodaran, E. Breckenfeld, A.K. Choquette, et al., Stabilization of mixed-phase structures in highly strained  $\text{BiFeO}_3$  thin films via chemical-alloying, *Appl. Phys. Lett.* **100**, 082904-4 (2012).

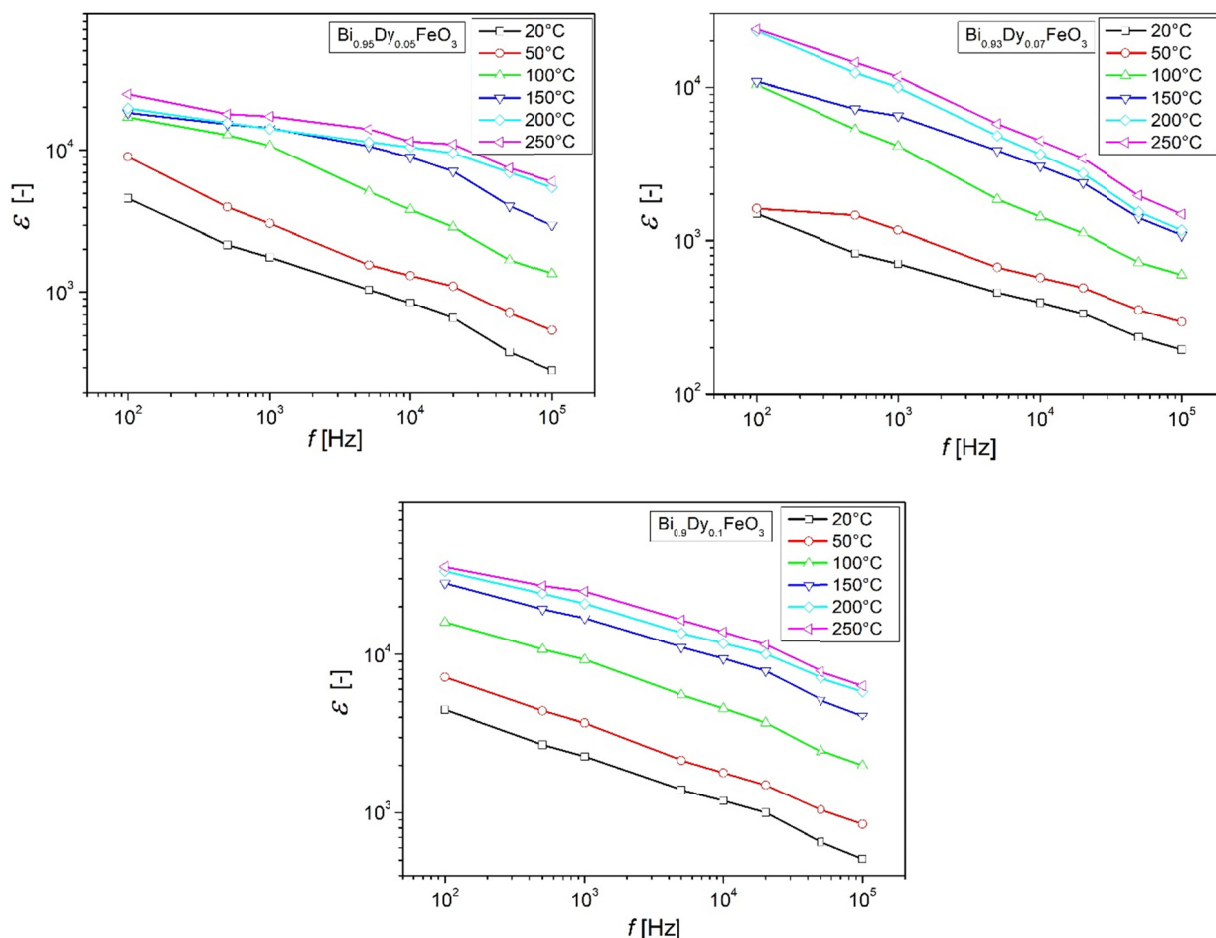


Fig. 6. Electric permeability  $\varepsilon$  as a function of frequency for the obtained ceramic samples

- [2] J.G. Wu, J. Wang, D.Q. Xiao, J.G. Zhu, A method to improve electrical properties of BiFeO<sub>3</sub> thin films, *ACS Appl. Mater. Inter.* **4**, 1182-1185 (2012)
- [3] W. Eerenstein, N.D. Mathur, J.F. Scott, Multiferroic and magnetoelectric materials, *Nature* **442**, (2006).
- [4] X. Qi, X. Zhang, X. Wang, H. Sun, J. Qi, Preparation and Properties of Dy doped La and Sc solution of BiFeO<sub>3</sub> Film, *Key Engineering Materials* **537**, 109-113 (2013).
- [5] S-H. Jo, S-G. Lee, S-H. Lee, Structural and pyroelectric properties of sol-gel derived multiferroic BFO thin films, *Materials Research Bulletin* **47**, 409-412 (2012).
- [6] D. Kothari, V.R. Reddy, A. Gupta, C. Meneghini, G. Aquilanti, Eu doping in multiferroic BiFeO<sub>3</sub> ceramics studied by Mossbauer and EXAFS spectroscopy, *J. Phys.: Condens. Matter* **22**, 356001 (2010).
- [7] R.A. Agarwal, S. Sanghi, et al., Rietveld analysis, dielectric and magnetic properties of Sr and Ti codoped BiFeO<sub>3</sub> multiferroic, *Journal Of Applied Physics* **110**, 073909 (2011).
- [8] G.S. Lotey, N.K. Verma, Multiferroism in rare earth metals-doped BiFeO<sub>3</sub> Nanowires, Superlattices and Microstructures **60**, 60-66 (2013).
- [9] J. Wang, M. Li, X. Liu, P. Pei, J. Liu, B. Yu, X. Zhao, Synthesis and ferroelectric properties of Nd doped multiferroic BiFeO<sub>3</sub> nanotubes, *Chin. Sci. Bull.* **55** (16), 1594-1597 (2010).
- [10] Z. Trzaska Durski, H. Trzaska Durska, *Podstawy krystalografii*, OW Politechniki Warszawskiej, Warszawa, s. 141-143 (2003).
- [11] S. Pattanayak, R.N.P. Choudhary, R. Piyush, S.R. Shan-nigrahi, Effect of Dy-substitution on structural, electrical and magnetic properties of multiferroic BiFeO<sub>3</sub> ceramics, *Ceramics International* **40**, 7983-7991 (2014).
- [12] L.M. Hrib, O.F. Caltun, Effects of the chemical composition of the magnetostrictive phase on the dielectric and magnetoelectric properties of cobalt ferrite-barium titanate composite, *Journal of Alloys and Compounds* **509**, 6644-6648 (2011).
- [13] S.S. Chougule, D.R. Patil, B.K. Chougule, Electrical conduction and magnetoelectric effect in ferroelectric rich (x) Ni<sub>0.9</sub>Zn<sub>0.1</sub>Fe<sub>2</sub>O<sub>4</sub>+(1-x)PZT ME composites, *Journal of Alloys and Compounds* **452**, 205-209 (2008).